Coupled-mode field computations for underwater canyons and ridges

Sven M. Ivansson[1]

[1]SE-11529 Stockholm, Sweden

Sven M. Ivansson, SE-11529 Stockholm, Sweden; sven.ivansson@gmail.com

Abstract: *Coupled-mode methods have been used in underwater acoustics to compute 3D sound propagation and scattering. Significant computational simplifications are possible for media with lateral variation restricted to cylindrical symmetry, and also for media which are invariant in one of the horizontal directions. For discrete coupled-modes, with a discretization of the medium into laterally homogeneous regions, ring regions for a cylindrically symmetric medium and strip regions for a medium that is invariant in one of the horizontal directions, the basic Helmholtz-equation modal solutions involve Bessel/Hankel functions and exponential functions, respectively. There is a summation over angular order in the ring-region case, and an integration over horizontal wavenumber in the strip-region case. The present paper explores the similarities between the two cases. With a reflection- (or scattering-) matrix formulation for modes, the equations for the strip-region case are derived as limits of the equations for the ring-region case when the symmetry axis of the medium tends to infinity. This alternative to a Fourier-transform derivation directly provides suitable basis functions to inherit reflection-matrix symmetry, and it emphasizes the usefulness of proposed Bessel/Hankel-function scalings. Focusing the strip-region case, the paper also includes mathematically exact field decompositions with partial waves having a natural physical interpretation. Such decompositions should be of interest for analysis of continuous-wave and broad-band results, as a complement to approximate ray methods. Reverberation operators for selected parts of the medium are expanded in terms of elementary R/T (reflection/transmission) matrices for the modes. The implementation is surprisingly convenient, using reflection-matrix recursions from both ends of the medium involving selected restarts with vanishing reflection matrices. Utilizing the elementary reflection matrices for stabilized back-propagation from the source and from selected reflection regions, to obtain partial-wave field-expansion coefficients in the different strip regions, it is not necessary to compute elementary transmission matrices explicitly. Examples for underwater canyons and ridges are given, including comparisons to previous approximate parabolic-equation results. It is instructive to plot elementary R/T-matrix columns as functions of horizontal wavenumber.*

Keywords: *wavenumber integration, reflection/transmission-matrices, partial waves*

1. MEDIUM INDEPENDENT OF THE HORIZONTAL *Y*-COORDINATE AS A LIMITING CASE OF A CYLINDRICALLY SYMMETRIC MEDIUM

Consider a fluid medium that is cylindrically symmetric around a vertical axis at $\mathbf{x} = (x, y, z) = (\xi, 0, 0)$ in a Cartesian xyz system with horizontal coordinates x,y and depth z. In the xy-plane, let $(r(x, y), \phi(x, y))$ denote polar coordinates centered at $(\xi, 0)$ The medium is laterally homogeneous in each of $N + 1$ ring regions, where region n=1,2,..,$N + 1$ for $x < \xi$ cuts the x-axis at the segments $x < x_1$, $x_1 < x < x_2$, .., $x_{N-1} < x < x_N$, and $x_N < x < \xi$, respectively. When ξ tends to $+\infty$ with fixed x_n, $n = 1, 2, .., N$, a y-independent medium appears, that is laterally homogeneous in each of $N + 1$ strip regions. Fig. 1 gives an illustration.

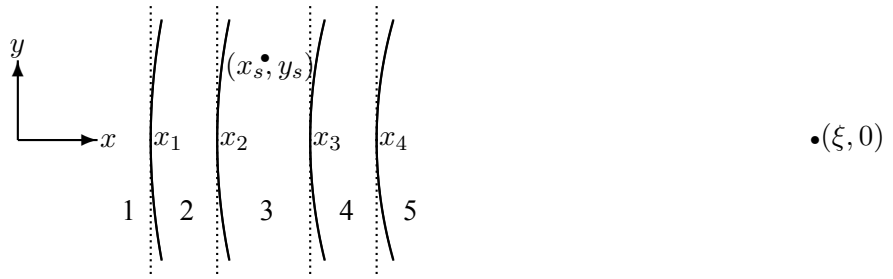

Figure 1: Horizontal xy-plane with laterally homogeneous ring regions for a cylindrically symmetric medium. The vertical symmetry axis is at $(x, y) = (\xi, 0)$. The dotted lines indicate the limiting strip regions when ξ tends to $+\infty$. Here, $N = 4$ and $n_s = 3$.

A symmetric time-harmonic point source, moment-tensor strength M, is at $\mathbf{x}_s = (x_s, y_s, z_s)$. With $\omega > 0$ as angular frequency and t as time, the (omitted) time factor is $\exp(-\mathrm{i}\omega t)$. Assuming large ξ, the source is in region n_s. With $r_s(x, y) = |(x, y) - (x_s, y_s)|$ and $a_{m,s} = -\mathrm{i}M\omega^2 Z_{m,n_s}(z_s)/4\lambda_{n_s}(z_s)$, the pressure $p(\mathbf{x})$ for $\mathbf{x}$ in region n is, cf. [1, Eqs. (8),(24)-(25)],

$$p(\mathbf{x}) = 2\sum_{\nu=0}^{+\infty} [\mathbf{\Phi}_n(\mathbf{x}) \cdot \mathbf{a}_n + \mathbf{\Psi}_n(\mathbf{x}) \cdot \mathbf{b}_n/\xi] \cos(\nu(\phi(x, y) - \phi(x_s, y_s))) \quad \text{and} \quad (1)$$

$$p(\mathbf{x}) = \sum_m a_{m,s} Z_{m,n_s}(z) \mathrm{H}_0^{(1)}(k_{m,n_s} r_s(x, y)) + 2\sum_{\nu=0}^{+\infty} [\mathbf{\Phi}_{n_s}(\mathbf{x}) \cdot \bar{\mathbf{a}}_{n_s} + \mathbf{\Psi}_{n_s}(\mathbf{x}) \cdot \mathbf{b}_{n_s}/\xi] \cos(\nu(\phi(x, y) - \phi(x_s, y_s))) \quad (2)$$

for $n \neq n_s$ and $n = n_s$, respectively. Even and odd parity terms are here combined, cf. [1, p. 1435], and ν=0,1,.. denotes azimuthal order. With some appropriate scalings for the current context, $\mathbf{a}_n = \{(a_n)_m\}$, $\mathbf{b}_n = \{(b_n)_m\}$, and $\bar{\mathbf{a}}_{n_s} = \{(\bar{a}_{n_s})_m\}$ are ν-dependent column vectors such that (except for dimensions) $\mathbf{a}_1 = \mathbf{0}$ when $n_s \neq 1$, $\mathbf{b}_{N+1} = \mathbf{0}$, and $\bar{\mathbf{a}}_{n_s} = \mathbf{0}$ when $n_s = 1$. Each region n has an artificial termination at depth involving absorption to avoid undesired reflections. With mode index m, $k_{m,n}$ and $Z_{m,n}(z)$ are modal horizontal wavenumbers and normalized (!) mode functions, respectively, while $\lambda_n(z)$ is the product of density and squared sound speed. For n=1,2,..,$N + 1$, the ν-dependent row vectors $\mathbf{\Phi}_n(\mathbf{x})$ and $\mathbf{\Psi}_n(\mathbf{x})$ for incoming and outgoing waves, respectively, are adapted from [1]. With the Kronecker delta $\delta_{\nu 0}$,

$$\mathbf{\Phi}_n(\mathbf{x}) = \{(\Phi_n(\mathbf{x}))_m\} \quad \text{with} \quad (\Phi_n(\mathbf{x}))_m = Z_{m,n}(z)\, \hat{\mathrm{J}}_{m,n}(r(x, y); \nu) \times (1 - \delta_{\nu 0}/2)^{1/2} \quad (3)$$

$$\mathbf{\Psi}_n(\mathbf{x}) = \{(\Psi_n(\mathbf{x}))_m\} \quad \text{with} \quad (\Psi_n(\mathbf{x}))_m = Z_{m,n}(z)\, \hat{\mathrm{H}}_{m,n}(r(x, y); \nu) \times (1 - \delta_{\nu 0}/2)^{1/2}. \quad (4)$$

Here, with $r_n = \xi - x_n$ for n=1,2,..,N, $r_0 = r_1$ and $r_{N+1} = r_N$,

$$\hat{\mathrm{J}}_{m,n}(r; \nu) = \mathrm{J}_\nu(k_{m,n} r) \mathrm{H}_\nu^{(1)}(k_{m,n} r_{n-1}) \quad \text{and} \quad \hat{\mathrm{H}}_{m,n}(r; \nu) = \frac{\mathrm{H}_\nu^{(1)}(k_{m,n} r)}{\mathrm{H}_\nu^{(1)}(k_{m,n} r_n)}\,. \quad (5)$$

The idea is now to consider large ξ and ν, which tend to $+\infty$ while the quotient between ν/ξ and κ, a positive real parameter, tends to 1. This is written $\nu/\xi \sim \kappa$. The following asymptotic relations follow from [2, 9.3.35-46,10.4.59,10.4.61], for derivations see [3] and [4, §11.10]:

$$\mathrm{J}_\nu(\nu\frac{k}{\kappa} - k\,\Delta x) \;\sim\; \frac{\exp(\mathrm{i}\pi/4)}{\sqrt{2\pi}}\,\frac{\sqrt{\kappa}}{(k^2-\kappa^2)^{1/4}}\,\frac{1}{\sqrt{\nu}}\;\mathrm{e}^{-\nu\,\Omega(k/\kappa)}\,\mathrm{e}^{+\mathrm{i}\,\Delta x\,\sqrt{k^2-\kappa^2}} \tag{6}$$

$$\mathrm{H}^{(1)}_\nu(\nu\frac{k}{\kappa} - k\,\Delta x) \;\sim\; 2\,\frac{\exp(-\mathrm{i}\pi/4)}{\sqrt{2\pi}}\,\frac{\sqrt{\kappa}}{(k^2-\kappa^2)^{1/4}}\,\frac{1}{\sqrt{\nu}}\;\mathrm{e}^{+\nu\,\Omega(k/\kappa)}\,\mathrm{e}^{-\mathrm{i}\,\Delta x\,\sqrt{k^2-\kappa^2}} \tag{7}$$

$$\mathrm{J}'_\nu(\nu\frac{k}{\kappa}) \;\sim\; \frac{\exp(-\mathrm{i}\pi/4)}{\sqrt{2\pi}}\,\frac{\kappa}{k}\,\frac{(k^2-\kappa^2)^{1/4}}{\sqrt{\kappa}}\,\frac{1}{\sqrt{\nu}}\;\mathrm{e}^{-\nu\,\Omega(k/\kappa)} \tag{8}$$

$$\left(\mathrm{H}^{(1)}_\nu\right)'(\nu\frac{k}{\kappa}) \;\sim\; 2\,\frac{\exp(\mathrm{i}\pi/4)}{\sqrt{2\pi}}\,\frac{\kappa}{k}\,\frac{(k^2-\kappa^2)^{1/4}}{\sqrt{\kappa}}\,\frac{1}{\sqrt{\nu}}\;\mathrm{e}^{+\nu\,\Omega(k/\kappa)} \tag{9}$$

where k is a wavenumber with a positive imaginary part, typically one of the $k_{m,n}$, and

$$\Omega(k/\kappa) \;=\; \int_{k/\kappa}^{1} \frac{\sqrt{1-s^2}}{s}\,ds\;. \tag{10}$$

To verify (6) and (7) for $\Delta x \neq 0$, note that $\nu\,\Omega(k/\kappa - k\,\Delta x/\nu) - \nu\,\Omega(k/\kappa) \;\sim\; -\mathrm{i}\,\Delta x\,\sqrt{k^2-\kappa^2}$.

With $x_0 = x_1$ and $x_{N+1} = x_N$, since $r(x,y) - \xi \sim r(x,y) - \nu/\kappa \sim -x$, (6)-(7) show that

$$\hat{\mathrm{J}}_{m,n}(r(x,y);\nu) \sim \tfrac{1}{\pi\sqrt{k^2-\kappa^2}}\,\tfrac{\kappa}{\nu}\,\hat{\mathrm{E}}^{(1)}_{m,n}(x;\kappa) \;\text{ and }\; \hat{\mathrm{H}}_{m,n}(r(x,y);\nu) \sim \hat{\mathrm{E}}^{(2)}_{m,n}(x;\kappa) \quad \text{where (11)}$$

$$\hat{\mathrm{E}}^{(1)}_{m,n}(x;\kappa) = \mathrm{e}^{+\mathrm{i}(x-x_{n-1})\sqrt{k^2_{m,n}-\kappa^2}} \quad \text{and} \quad \hat{\mathrm{E}}^{(2)}_{m,n}(x;\kappa) = \mathrm{e}^{-\mathrm{i}(x-x_n)\sqrt{k^2_{m,n}-\kappa^2}}\;. \tag{12}$$

Noting that $\phi(x,y) - \pi \sim -\kappa y/\nu$, $\cos(\nu(\phi(x,y) - \phi(x_s,y_s))) \;\sim\; \cos(\kappa(y-y_s))$. It follows that the asymptotic versions of (1) and (2), furnishing $p(\mathbf{x})$ for the y-independent medium, are

$$p(\mathbf{x}) \;\sim\; 2\int_0^{+\infty} [\mathbf{\Phi}_n(x,z)\cdot\mathbf{a}_n + \mathbf{\Psi}_n(x,z)\cdot\mathbf{b}_n]\cos(\kappa(y-y_s))\,d\kappa \qquad \text{and} \tag{13}$$

$$\begin{aligned} p(\mathbf{x}) \;\sim\; & \sum_m a_{m,s} Z_{m,n_s}(z)\mathrm{H}^{(1)}_0(k_{m,n_s} r_s(x,y)) \\ & + 2\int_0^{+\infty} [\mathbf{\Phi}_{n_s}(x,z)\cdot\bar{\mathbf{a}}_{n_s} + \mathbf{\Psi}_{n_s}(x,z)\cdot\mathbf{b}_{n_s}]\cos(\kappa(y-y_s))\,d\kappa\;, \end{aligned} \tag{14}$$

respectively. View κ as the part along the coordinate y of the horizontal modal wavenumbers $k_{m,n}$. Note the important **b**-vector scaling in (1)-(2), and that $d\kappa \sim 1/\xi \sim \kappa/\nu$. By (12), the contributions to the integrals in (13)-(14) from $\kappa >> \max_{m,n} \mathrm{Re}(k_{m,n})$ are small, as are the contributions to the sums in (1)-(2) from $\nu >> \xi\ \max_{m,n} \mathrm{Re}(k_{m,n})$ [1]. By forthcoming equations, the vectors $\mathbf{a}_n$, $\mathbf{b}_n$, and $\bar{\mathbf{a}}_{n_s}$ have finite κ-dependent asymptotic limits, typically nonvanishing. Apparently,

$$\xi\,\mathbf{\Phi}_n(\mathbf{x}) \sim \mathbf{\Phi}_n(x,z) \quad \text{and} \quad \mathbf{\Psi}_n(\mathbf{x}) \sim \mathbf{\Psi}_n(x,z)\;, \tag{15}$$

where the κ-dependent row vectors $\mathbf{\Phi}_n(x,z) = \{(\Phi_n(x,z))_m\}$ and $\mathbf{\Psi}_n(x,z) = \{(\Psi_n(x,z))_m\}$, not to be confused with $\mathbf{\Phi}_n(\mathbf{x})$ and $\mathbf{\Psi}_n(\mathbf{x})$, are as in [5, Eqs. (30)-(33)].

In terms of reflection matrices $\mathbf{R}_n$ with elements $(R_n)_{m;m'}$ and $\bar{\mathbf{R}}_n$ with elements $(\bar{R}_n)_{m;m'}$,

$$\mathbf{b}_n = \mathbf{R}_n\cdot\hat{\mathbf{H}}_n\cdot\mathbf{a}_n \;\text{ for } n > n_s \quad \text{and} \quad \mathbf{a}_n = \bar{\mathbf{R}}_n\cdot\hat{\mathbf{H}}_n\cdot\mathbf{b}_n \;\text{ for } n < n_s\;. \tag{16}$$

To relate to [1, Eqs. (16),(30)], note that $\mathbf{b}_n/\xi = (\mathbf{R}_n/\xi)\cdot\hat{\mathbf{H}}_n\cdot\mathbf{a}_n$ and $\mathbf{a}_n = (\xi\,\bar{\mathbf{R}}_n)\cdot\hat{\mathbf{H}}_n\cdot(\mathbf{b}_n/\xi)$. $\hat{\mathbf{H}}_n = \mathrm{diag}_m\left(\hat{\mathrm{H}}_{m,n}(r_{n-1};\nu)\right)$, a diagonal matrix in m. $\hat{\mathbf{H}}_1 = \hat{\mathbf{H}}_{N+1} = \mathbf{I}$. Considering the sides of the source region, at $r_s(x,y) = r_{n_s}$ when $n_s \neq N+1$ and $r_s(x,y) = r_{n_{s-1}}$ when $n_s \neq 1$,

$$\mathbf{b}_{n_s} = \mathbf{R}_{n_s}\cdot\mathbf{a}_{n_s} \quad \text{and} \quad \bar{\mathbf{a}}_{n_s} = \bar{\mathbf{R}}_{n_s}\cdot\bar{\mathbf{b}}_{n_s}\;. \tag{17}$$

$\mathbf{R}_{n_s}$ and $\bar{\mathbf{R}}_{n_s}$ are also reflection matrices, $\mathbf{R}_{n_s}=\mathbf{0}$ when $n_s=N+1$ and $\bar{\mathbf{R}}_{n_s}=\mathbf{0}$ when $n_s=1$, while $\mathbf{a}_{n_s}=\{(a_{n_s})_m\}$ and $\bar{\mathbf{b}}_{n_s}=\{(\bar{b}_{n_s})_m\}$ are additional ν-dependent column vectors:

$$\mathbf{a}_{n_s}=\hat{\mathbf{H}}_{n_s}\cdot\bar{\mathbf{a}}_{n_s}-\frac{\mathrm{i}M\omega^2}{4\,\lambda_{n_s}(z_s)}\mathbf{\Psi}^{\mathrm{T}}_{n_s}(\mathbf{x}_s)\quad\text{and}\quad\bar{\mathbf{b}}_{n_s}=\hat{\mathbf{H}}_{n_s}\cdot\mathbf{b}_{n_s}-\frac{\mathrm{i}M\omega^2}{4\,\lambda_{n_s}(z_s)}\xi\,\mathbf{\Phi}^{\mathrm{T}}_{n_s}(\mathbf{x}_s)\,,\quad(18)$$

as adapted from [1, Eqs. (29),(32)]. Note the factor ξ because of the **b**-vector scaling in (1)-(2).

Continuity conditions at the region interfaces show that, cf. [1, Eqs. (17),(35)-(36)],

$$\mathbf{a}_{n_s+1}=\mathbf{A}_{n_s}\cdot\mathbf{a}_{n_s}+\mathbf{B}_{n_s}\cdot\mathbf{b}_{n_s}\;\&\;\hat{\mathbf{H}}_{n_s+1}\cdot\mathbf{b}_{n_s+1}=\mathbf{C}_{n_s}\cdot\mathbf{a}_{n_s}+\mathbf{D}_{n_s}\cdot\mathbf{b}_{n_s}\quad\text{if } n_s\le N,\quad(19)$$

$$\mathbf{a}_{n+1}=\mathbf{A}_{n}\cdot\hat{\mathbf{H}}_{n}\cdot\mathbf{a}_{n}+\mathbf{B}_{n}\cdot\mathbf{b}_{n}\;\&\;\hat{\mathbf{H}}_{n+1}\cdot\mathbf{b}_{n+1}=\mathbf{C}_{n}\cdot\hat{\mathbf{H}}_{n}\cdot\mathbf{a}_{n}+\mathbf{D}_{n}\cdot\mathbf{b}_{n}\quad\text{if } n_s<n\le N,\quad(20)$$

$$\mathbf{b}_{n_s-1}=\bar{\mathbf{A}}_{n_s}\cdot\bar{\mathbf{b}}_{n_s}+\bar{\mathbf{B}}_{n_s}\cdot\bar{\mathbf{a}}_{n_s}\;\&\;\hat{\mathbf{H}}_{n_s-1}\cdot\mathbf{a}_{n_s-1}=\bar{\mathbf{C}}_{n_s}\cdot\bar{\mathbf{b}}_{n_s}+\bar{\mathbf{D}}_{n_s}\cdot\bar{\mathbf{a}}_{n_s}\quad\text{if } n_s>1,\quad(21)$$

$$\mathbf{b}_{n-1}=\bar{\mathbf{A}}_{n}\cdot\hat{\mathbf{H}}_{n}\cdot\mathbf{b}_{n}+\bar{\mathbf{B}}_{n}\cdot\mathbf{a}_{n}\;\&\;\hat{\mathbf{H}}_{n-1}\cdot\mathbf{a}_{n-1}=\bar{\mathbf{C}}_{n}\cdot\hat{\mathbf{H}}_{n}\cdot\mathbf{b}_{n}+\bar{\mathbf{D}}_{n}\cdot\mathbf{a}_{n}\quad\text{if } 1<n<n_s.\quad(22)$$

Here, $\mathbf{A}_n$,$\mathbf{B}_n$,$\mathbf{C}_n$,$\mathbf{D}_n$ and $\bar{\mathbf{A}}_n$,$\bar{\mathbf{B}}_n$,$\bar{\mathbf{C}}_n$,$\bar{\mathbf{D}}_n$ are as in [1] but with $\mathbf{B}_n$,$\bar{\mathbf{C}}_n$ divided by ξ and $\mathbf{C}_n$,$\bar{\mathbf{B}}_n$ multiplied by ξ. Certain matrices $\hat{\mathbf{J}}^+_n$, $\tilde{\mathbf{J}}^+_n$, $\hat{\mathbf{J}}^-_n$, $\tilde{\mathbf{J}}^-_n$, $\mathbf{E}^+_n$, $\mathbf{E}^-_n$, $\mathbf{\Lambda}_n$, and $\bar{\mathbf{\Lambda}}_n$, are involved [1].

Starting from $\mathbf{R}_{N+1}=\mathbf{0}$ and $\bar{\mathbf{R}}_1=\mathbf{0}$, (19)-(22) provide recursions, cf. [1, Eqs. (20),(39)],

$$\mathbf{R}_n=-(\mathbf{D}_n-\hat{\mathbf{H}}_{n+1}\cdot\mathbf{R}_{n+1}\cdot\hat{\mathbf{H}}_{n+1}\cdot\mathbf{B}_n)^{-1}\cdot(\mathbf{C}_n-\hat{\mathbf{H}}_{n+1}\cdot\mathbf{R}_{n+1}\cdot\hat{\mathbf{H}}_{n+1}\cdot\mathbf{A}_n)\quad(23)$$

$$\bar{\mathbf{R}}_n=-(\bar{\mathbf{D}}_n-\hat{\mathbf{H}}_{n-1}\cdot\bar{\mathbf{R}}_{n-1}\cdot\hat{\mathbf{H}}_{n-1}\cdot\bar{\mathbf{B}}_n)^{-1}\cdot(\bar{\mathbf{C}}_n-\hat{\mathbf{H}}_{n-1}\cdot\bar{\mathbf{R}}_{n-1}\cdot\hat{\mathbf{H}}_{n-1}\cdot\bar{\mathbf{A}}_n)\,.\quad(24)$$

Turning to asymptotic relations, (6)-(9) and (11)-(12) show that

$$\hat{\mathbf{H}}_n\sim\hat{\mathbf{E}}_n=\mathrm{diag}_m\left(\hat{\mathrm{E}}^{(1)}_{m,n}(x_n;\kappa)\right)=\mathrm{diag}_m\left(\hat{\mathrm{E}}^{(2)}_{m,n}(x_{n-1};\kappa)\right)$$

$$\hat{\mathbf{J}}^+_n\sim\hat{\mathbf{J}}^-_n\sim\tfrac{\kappa}{\nu}\left(\mathrm{diag}_m(\pi(k^2_{m,n}-\kappa^2)^{1/2})\right)^{-1}\quad\text{and}\quad\tilde{\mathbf{J}}^+_n\sim\tilde{\mathbf{J}}^-_n\sim\tfrac{\kappa}{\nu}\left(\mathrm{diag}_m(\pi k_{m,n})\right)^{-1}$$

$$\mathbf{E}^+_n\sim\mathbf{E}^-_n\sim\mathrm{diag}_m\left(\tfrac{(k^2_{m,n}-\kappa^2)^{1/2}}{k_{m,n}}\right)\quad\text{and}\quad\mathbf{\Lambda}_n\sim\bar{\mathbf{\Lambda}}_n\sim\tfrac{\pi}{2}\,\tfrac{\nu}{\kappa}\,\mathrm{diag}_m(k_{m,n})\,.$$

With $\mathbf{K}_n=\mathrm{diag}_m(\pi(k^2_{m,n}-\kappa^2)^{1/2})$, and $\mathbf{F}_n$,$\mathbf{G}_n$ and $\bar{\mathbf{F}}_n$ and $\bar{\mathbf{G}}_n$ as in [1, Eqs. (18)-(19),(37)-(38)], but (!) with $(k^2_{m',n}-\kappa^2)^{1/2}/(k^2_{m,n+1}-\kappa^2)^{1/2}$ replacing $k_{m',n}/k_{m,n+1}$ in $\mathbf{G}_n$ and $(k^2_{m',n}-\kappa^2)^{1/2}/(k^2_{m,n-1}-\kappa^2)^{1/2}$ replacing $k_{m',n}/k_{m,n-1}$ in $\bar{\mathbf{G}}_n$,

$$\mathbf{A}_n\sim\mathbf{K}_{n+1}\cdot\tfrac{\mathbf{F}_n+\mathbf{G}_n}{2}\cdot\mathbf{K}_n^{-1}\,,\;\mathbf{B}_n\sim\mathbf{K}_{n+1}\cdot\tfrac{\mathbf{F}_n-\mathbf{G}_n}{2}\,,\;\mathbf{C}_n\sim\tfrac{\mathbf{F}_n-\mathbf{G}_n}{2}\cdot\mathbf{K}_n^{-1}\,,\;\mathbf{D}_n\sim\tfrac{\mathbf{F}_n+\mathbf{G}_n}{2}\,,\quad(25)$$

$$\bar{\mathbf{A}}_n\sim\tfrac{\bar{\mathbf{F}}_n+\bar{\mathbf{G}}_n}{2}\,,\;\bar{\mathbf{B}}_n\sim\tfrac{\bar{\mathbf{F}}_n-\bar{\mathbf{G}}_n}{2}\cdot\mathbf{K}_n^{-1}\,,\;\bar{\mathbf{C}}_n\sim\mathbf{K}_{n-1}\cdot\tfrac{\bar{\mathbf{F}}_n-\bar{\mathbf{G}}_n}{2}\,,\;\bar{\mathbf{D}}_n\sim\mathbf{K}_{n-1}\cdot\tfrac{\bar{\mathbf{F}}_n+\bar{\mathbf{G}}_n}{2}\cdot\mathbf{K}_n^{-1}\,.\quad(26)$$

Insertion of these relations, and $\hat{\mathbf{H}}_n\sim\hat{\mathbf{E}}_n$, into (23)-(24) provides recursions for the asymptotic versions of the reflection matrices, valid for the y-independent medium. It follows that $\mathbf{R}_n$ and $\bar{\mathbf{R}}_n$ have finite κ-dependent asymptotic limits as ξ and ν tend to $+\infty$. Since $\mathbf{R}_n$ and $\bar{\mathbf{R}}_n$ are symmetric, [1, Sec. V A], their asymptotic versions are also symmetric. The transmission-matrix relations according to [1, Eqs. (42)-(44)] have obvious asymptotic correspondences.

By (15) and since $\hat{\mathbf{H}}_n\sim\hat{\mathbf{E}}_n$, the asymptotic version of (18) is, cf. [5, Eqs. (37)-(38)],

$$\mathbf{a}_{n_s}=\hat{\mathbf{E}}_{n_s}\cdot\bar{\mathbf{a}}_{n_s}-\frac{\mathrm{i}M\omega^2}{4\,\lambda_{n_s}(z_s)}\mathbf{\Psi}^{\mathrm{T}}_{n_s}(x_s,z_s)\quad\text{and}\quad\bar{\mathbf{b}}_{n_s}=\hat{\mathbf{E}}_{n_s}\cdot\mathbf{b}_{n_s}-\frac{\mathrm{i}M\omega^2}{4\,\lambda_{n_s}(z_s)}\mathbf{\Phi}^{\mathrm{T}}_{n_s}(x_s,z_s)\,.\quad(27)$$

Solution of an equation system provides [5, Eqs. (39)-(40)], (17) then yields $\mathbf{b}_{n_s}$ and $\bar{\mathbf{a}}_{n_s}$.

For the y-independent medium, stabilized back-propagation using asymptotic versions of (19)-(22) and (16)-(17) give the remaining $\mathbf{a}_{n_s}$ and $\mathbf{b}_{n_s}$. Specifically, cf. [1, Eqs. (23),(40)]:

$$\mathbf{a}_{n_s+1}=\mathbf{A}_{n_s}\cdot\mathbf{a}_{n_s}+\mathbf{B}_{n_s}\cdot\mathbf{b}_{n_s}\quad\text{and}\quad\mathbf{b}_{n_s+1}=\mathbf{R}_{n_s+1}\cdot\hat{\mathbf{E}}_{n_s+1}\cdot\mathbf{a}_{n_s+1}\quad\text{when } n_s\le N,\quad(28)$$

$$\mathbf{a}_{n+1}=\mathbf{A}_{n}\cdot\hat{\mathbf{E}}_{n}\cdot\mathbf{a}_{n}+\mathbf{B}_{n}\cdot\mathbf{b}_{n}\quad\text{and}\quad\mathbf{b}_{n+1}=\mathbf{R}_{n+1}\cdot\hat{\mathbf{E}}_{n+1}\cdot\mathbf{a}_{n+1}\quad\text{for } n_s<n\le N,\quad(29)$$

$$\mathbf{b}_{n_s-1}=\bar{\mathbf{A}}_{n_s}\cdot\bar{\mathbf{b}}_{n_s}+\bar{\mathbf{B}}_{n_s}\cdot\bar{\mathbf{a}}_{n_s}\quad\text{and}\quad\mathbf{a}_{n_s-1}=\bar{\mathbf{R}}_{n_s-1}\cdot\hat{\mathbf{E}}_{n_s-1}\cdot\mathbf{b}_{n_s-1}\quad\text{when } n_s>1,\quad(30)$$

$$\mathbf{b}_{n-1}=\bar{\mathbf{A}}_{n}\cdot\hat{\mathbf{E}}_{n}\cdot\mathbf{b}_{n}+\bar{\mathbf{B}}_{n}\cdot\mathbf{a}_{n}\quad\text{and}\quad\mathbf{a}_{n-1}=\bar{\mathbf{R}}_{n-1}\cdot\hat{\mathbf{E}}_{n-1}\cdot\mathbf{b}_{n-1}\quad\text{for } 1<n<n_s,\quad(31)$$

with insertion of the asymptotic reflection matrices, $\hat{\mathbf{H}}_n \sim \hat{\mathbf{E}}_n$, and (25)-(26). Transmission matrices analogous to those in [1, Sec. V A] follow from (16)-(17) and (28)-(31) by writing $\mathbf{a}_{n_s+1} = (\mathbf{A}_{n_s} + \mathbf{B}_{n_s} \cdot \mathbf{R}_{n_s}) \cdot \mathbf{a}_{n_s}$ when $n_s \leq N$, $\mathbf{a}_{n+1} = (\mathbf{A}_n + \mathbf{B}_n \cdot \mathbf{R}_n) \cdot \hat{\mathbf{E}}_n \cdot \mathbf{a}_n$ for $n_s < n \leq N$, $\mathbf{b}_{n_s-1} = (\bar{\mathbf{A}}_{n_s} + \bar{\mathbf{B}}_{n_s} \cdot \bar{\mathbf{R}}_{n_s}) \cdot \bar{\mathbf{b}}_{n_s}$ when $n_s > 1$, and $\mathbf{b}_{n-1} = (\bar{\mathbf{A}}_n + \bar{\mathbf{B}}_n \cdot \hat{\mathbf{R}}_n) \cdot \hat{\mathbf{E}}_n \cdot \mathbf{b}_n$ for $1 < n < n_s$.

An alternative expression for the initial mode sum in (2) and (14) appears as

$$\tfrac{-\mathrm{i}M\omega^2}{4\,\lambda_{n_s}(z_s)}\, 2 \int_0^{+\infty} \Big[\mathbf{\Phi}_{n_s}(x,z) \cdot \hat{\mathbf{E}}_{n_s}^{-1} \cdot \mathbf{\Psi}_{n_s}^{\mathrm{T}}(x_s,z_s) \Big] \cos(\kappa(y-y_s))\, d\kappa \quad \text{for } x > x_s \tag{32}$$

$$\tfrac{-\mathrm{i}M\omega^2}{4\,\lambda_{n_s}(z_s)}\, 2 \int_0^{+\infty} \Big[\mathbf{\Psi}_{n_s}(x,z) \cdot \hat{\mathbf{E}}_{n_s}^{-1} \cdot \mathbf{\Phi}_{n_s}^{\mathrm{T}}(x_s,z_s) \Big] \cos(\kappa(y-y_s))\, d\kappa \quad \text{for } x < x_s\,. \tag{33}$$

Letting ξ and ν tend to $+\infty$, this follows from the asymptotic versions of [1, Eqs. (27)-(28)], using $\hat{\mathbf{H}}_n \sim \hat{\mathbf{E}}_n$ and (15) together with $d\kappa \sim 1/\xi$. Note the factor 2 in (32)-(33), because $\mathbf{\Phi}_n(\mathbf{x})$ and $\mathbf{\Psi}_n(\mathbf{x})$ are $2^{1/2}$ times as large in [1] than here. A derivation of (27) directly from (32)-(33) and (14) is possible by changing "x reference" between the sides of the source region. Uniqueness of a mode expansion verifies the Fourier-transform relation

$$\mathrm{H}_0^{(1)}(k\sqrt{x^2+y^2}) = \frac{2}{\pi} \int_0^{+\infty} \frac{\exp(\mathrm{i}|x|\sqrt{k^2-\kappa^2})}{\sqrt{k^2-\kappa^2}} \cos(\kappa y)\, d\kappa\,. \tag{34}$$

Here, $k \neq 0$ and $\sqrt{k^2-\kappa^2}$ are wavenumbers (nonnegative imaginary parts, not negative real).

The asymptotic relations (11) confirm usefulness of the scalings of $\mathrm{J}_\nu(k_{m,n}r)$ and $\mathrm{H}_\nu^{(1)}(k_{m,n}r)$ in the definitions of $\mathbf{\Phi}_n(\mathbf{x})$ and $\mathbf{\Psi}_n(\mathbf{x})$, respectively, according to (3)-(5). Moreover, the factor $(\pi\sqrt{k^2-\kappa^2})^{-1}$ in the first relation (11) explains the appearance of a corresponding factor in the definition of $\mathbf{\Phi}_n(x,z)$ according to [5, Eqs. (30)-(33)] and the role of this factor to forward symmetric reflection matrices $\mathbf{R}_n$,$\bar{\mathbf{R}}_n$ to the y-independent medium.

2. FIELD DECOMPOSITION INTO PARTIAL WAVES

For the source region of a y-independent medium, consider (14) together with [5, Eqs. (39)-(40)] and (17) for the relevant κ-dependent column vectors. View $\mathbf{a}_{n_s}$ as an excitation of the medium to the right of the source region (larger x), with response $\mathbf{b}_{n_s}$, and $\bar{\mathbf{b}}_{n_s}$ as an excitation of the medium to the left of the source region (smaller x), with response $\bar{\mathbf{a}}_{n_s}$. The matrix inverses in [5, Eqs. (39)-(40)] can be expanded in geometric series and interpreted as reverberation operators. Obviously, the parts $(-\mathrm{i}M\omega^2/4\lambda_{n_s}(z_s))\mathbf{\Psi}_{n_s}^{\mathrm{T}}(x_s,z_s)$ and $(-\mathrm{i}M\omega^2/4\lambda_{n_s}(z_s))\mathbf{\Phi}_{n_s}^{\mathrm{T}}(x_s,z_s)$ of $\mathbf{a}_{n_s}$ and $\bar{\mathbf{b}}_{n_s}$, respectively, provide the primary excitations. The remaining terms arise from reflections and reverberation within the source region. To proceed, regard each source-free region sequence between two x coordinates, for each κ, as a two-port with input field vectors $\mathbf{a}$ and $\bar{\mathbf{b}}$ from the left and right, respectively, and corresponding output field vectors $\mathbf{b}$ and $\bar{\mathbf{a}}$ at the left and right ends, respectively. With reflection matrices $\mathbf{R}$,$\bar{\mathbf{R}}$ and transmission matrices $\mathbf{T}$,$\bar{\mathbf{T}}$,

$$\mathbf{b} = \mathbf{R} \cdot \mathbf{a} + \bar{\mathbf{T}} \cdot \bar{\mathbf{b}} \quad \text{and} \quad \bar{\mathbf{a}} = \mathbf{T} \cdot \mathbf{a} + \bar{\mathbf{R}} \cdot \bar{\mathbf{b}}\,, \tag{35}$$

cf. (17). With the mode normalization and the basis functions $\mathbf{\Phi}(x,z)$,$\mathbf{\Psi}(x,z)$ according to [5, Eqs. (30)-(33)], the reflection matrices are symmetric and $\bar{\mathbf{T}} = \mathbf{T}^{\mathrm{T}}$; see [5, Sec. VI].

Next, consider two source-free region sequences of the y-independent medium, denoted A and B, connected by a source-free laterally homogeneous strip region. The corresponding κ-dependent R/T matrices are $\mathbf{R}_A$,$\bar{\mathbf{R}}_A$,$\mathbf{T}_A$,$\bar{\mathbf{T}}_A$ and $\mathbf{R}_B$,$\bar{\mathbf{R}}_B$,$\mathbf{T}_B$,$\bar{\mathbf{T}}_B$, respectively, and $\hat{\mathbf{E}}$ denotes the diagonal transmission matrix of the intermediate connection strip. Fig. 2 illustrates this composite structure, with input field vectors $\mathbf{a}$ and $\bar{\mathbf{b}}$, output field vectors $\mathbf{b}$ and $\bar{\mathbf{a}}$, and κ-dependent field vectors $\mathbf{a}^c$ and $\mathbf{b}^c$ of the connection strip, cf. (13). Lateral homogeneity of the connection

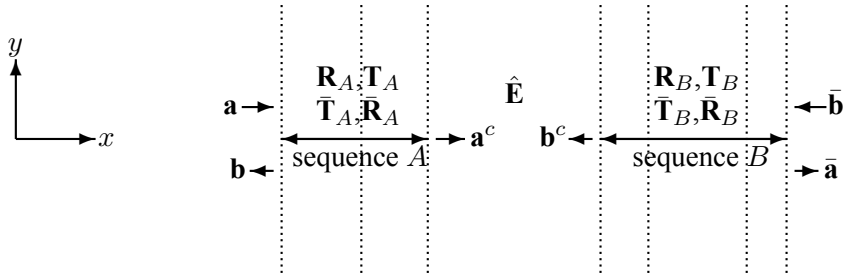

Figure 2: Horizontal xy-plane with two source-free region sequences, A and B, with a source-free connection strip in between. R/T matrices, input and output field vectors, as well as intermediate field vectors for the connection strip are indicated; all κ-dependent.

strip allows unambiguous specification, for each κ, of x-direction for the waves there. For the application to a particular partial wave, only one of $\mathbf{a}$ and $\bar{\mathbf{b}}$ is nonvanishing.

By addition rules for R/T matrices, cf. [6, Sec. 6.1], one obtains

$$\mathbf{R} = \mathbf{R}_A + \bar{\mathbf{T}}_A \cdot \hat{\mathbf{E}} \cdot \mathbf{R}_B \cdot \hat{\mathbf{E}} \cdot \left(\mathbf{I} - \bar{\mathbf{R}}_A \cdot \hat{\mathbf{E}} \cdot \mathbf{R}_B \cdot \hat{\mathbf{E}}\right)^{-1} \cdot \mathbf{T}_A \,, \tag{36}$$

$$\mathbf{T} = \mathbf{T}_B \cdot \left(\mathbf{I} - \hat{\mathbf{E}} \cdot \bar{\mathbf{R}}_A \cdot \hat{\mathbf{E}} \cdot \mathbf{R}_B\right)^{-1} \cdot \hat{\mathbf{E}} \cdot \mathbf{T}_A = \mathbf{T}_B \cdot \hat{\mathbf{E}} \cdot \left(\mathbf{I} - \bar{\mathbf{R}}_A \cdot \hat{\mathbf{E}} \cdot \mathbf{R}_B \cdot \hat{\mathbf{E}}\right)^{-1} \cdot \mathbf{T}_A \,, \tag{37}$$

$$\bar{\mathbf{R}} = \bar{\mathbf{R}}_B + \mathbf{T}_B \cdot \hat{\mathbf{E}} \cdot \bar{\mathbf{R}}_A \cdot \hat{\mathbf{E}} \cdot \left(\mathbf{I} - \mathbf{R}_B \cdot \hat{\mathbf{E}} \cdot \bar{\mathbf{R}}_A \cdot \hat{\mathbf{E}}\right)^{-1} \cdot \bar{\mathbf{T}}_B \,, \tag{38}$$

$$\bar{\mathbf{T}} = \bar{\mathbf{T}}_A \cdot \left(\mathbf{I} - \hat{\mathbf{E}} \cdot \mathbf{R}_B \cdot \hat{\mathbf{E}} \cdot \bar{\mathbf{R}}_A\right)^{-1} \cdot \hat{\mathbf{E}} \cdot \bar{\mathbf{T}}_B = \bar{\mathbf{T}}_A \cdot \hat{\mathbf{E}} \cdot \left(\mathbf{I} - \mathbf{R}_B \cdot \hat{\mathbf{E}} \cdot \bar{\mathbf{R}}_A \cdot \hat{\mathbf{E}}\right)^{-1} \cdot \bar{\mathbf{T}}_B \,. \tag{39}$$

Moreover, $\mathbf{a}^c = \mathbf{T}_A \cdot \mathbf{a} + \bar{\mathbf{R}}_A \cdot \hat{\mathbf{E}} \cdot \mathbf{b}^c$ and $\mathbf{b}^c = \bar{\mathbf{T}}_B \cdot \bar{\mathbf{b}} + \mathbf{R}_B \cdot \hat{\mathbf{E}} \cdot \mathbf{a}^c$. It follows that

$$\mathbf{a}^c = \left(\mathbf{I} - \bar{\mathbf{R}}_A \cdot \hat{\mathbf{E}} \cdot \mathbf{R}_B \cdot \hat{\mathbf{E}}\right)^{-1} \cdot \left(\mathbf{T}_A \cdot \mathbf{a} + \bar{\mathbf{R}}_A \cdot \hat{\mathbf{E}} \cdot \bar{\mathbf{T}}_B \cdot \bar{\mathbf{b}}\right) \tag{40}$$

$$\mathbf{b}^c = \left(\mathbf{I} - \mathbf{R}_B \cdot \hat{\mathbf{E}} \cdot \bar{\mathbf{R}}_A \cdot \hat{\mathbf{E}}\right)^{-1} \cdot \left(\bar{\mathbf{T}}_B \cdot \bar{\mathbf{b}} + \mathbf{R}_B \cdot \hat{\mathbf{E}} \cdot \mathbf{T}_A \cdot \mathbf{a}\right) \,. \tag{41}$$

With several region sequences A, B, C, .., and laterally homogeneous connection strips in between, recursive application of (36)-(39) provides R/T matrices for the composite structure in terms of elementary R/T matrices for the individual region sequences and diagonal transmission matrices for the connection strips. Starting from [5, Eqs. (39)-(40)], expansion of all inverse matrices yields the partial waves. Consider the source strip n_s as a special connection strip. Concerning $\mathbf{S}_{n_s} = \hat{\mathbf{E}}_{n_s} \cdot \mathbf{R}_{n_s}$ and $\bar{\mathbf{S}}_{n_s} = \hat{\mathbf{E}}_{n_s} \cdot \bar{\mathbf{R}}_{n_s}$ appearing in [5, Eqs. (39)-(40)], the resulting primary $\mathbf{R}_{n_s}$ and $\bar{\mathbf{R}}_{n_s}$ are the corresponding elementary reflection matrices for the region sequences immediately surrounding the source region. For each source-free connection strip, (40)-(41) with the elementary R/T matrices for the immediately surrounding region sequences as the pertinent $\mathbf{R}_A$,$\bar{\mathbf{R}}_A$,$\mathbf{T}_A$,$\bar{\mathbf{T}}_A$ and $\mathbf{R}_B$,$\bar{\mathbf{R}}_B$,$\mathbf{T}_B$,$\bar{\mathbf{T}}_B$ provide the field components there. With $\mathbf{a}^c = \mathbf{0}$ or $\mathbf{b}^c = \mathbf{0}$, a "connection strip" could be a source-free end strip of the medium, to the left or to the right. Integrations over κ are involved for each partial wave, cf. (13)-(14).

It is easy to adapt a computer program for computation of the whole field to computation of partial waves for specified laterally homogeneous connection strips, including the source region, and corresponding region sequences. Apply the reflection-matrix recursions according to (23) and (24), from $n = N$ to 1 and from $n = 2$ to $N + 1$, respectively. In this process, restart the recursion with a zero reflection matrix in the right-hand side upon entry to a region sequence from one of the specified connection strips. This gives the elementary reflection matrices $\mathbf{R}_A$,$\mathbf{R}_B$,.. and $\bar{\mathbf{R}}_A$,$\bar{\mathbf{R}}_B$,.. for the region sequences. It is not necessary to compute the (elementary) transmission matrices explicitly. Typically, transmission is best handled by sequential matrix-vector multiplications according to the technique with stabilized back-propagation; cf. (28)-(31).

For specified region sequences A,B,C,.. and corresponding laterally homogeneous connection strips in between, there is a basic partial wave p^0 and additional partial waves $p_{j_l,..,j_2,j_1}$. Here, $l \geq 1$ and $j_1, j_2, .., j_l$ denote region sequences (A,B,..). In the source region n_s, p^0 agrees with the incident wave there, i.e., the initial mode sum in (14). Transmission to the left and to the right yields p^0 in the other connection strips and in the region sequences. Transmission into a region sequence is done as usual, with stabilized sequential matrix-vector multiplications; cf. (28)-(31). The corresponding backward-going waves in the region sequence are thereby included. Transmitted from the source region in the same way, the additional partial wave $p_{j_l,..,j_2,j_1}$ appears by reflections from the region sequences $j_1, j_2, .., j_l$, in this order, and transmission from there. The backward-going waves in the traversed region sequences are again included. The total field in a particular region sequence or connection strip appears by summing all partial waves which contribute to the field there.

There is an analogous development for a cylindrically symmetric medium, with summation over ν instead of integration over κ [(1)-(2) instead of (13)-(14)] and with $\hat{\mathbf{H}}$ instead of $\hat{\mathbf{E}}$.

3. CANYON EXAMPLES

Fig. 3 shows coupled-mode results for a Gaussian canyon, water sound-speed 1.5 km/s, with good agreement to the two most accurate 3D PE (parabolic-equation) solutions in [7, Fig. 6]. There are 720 laterally homogeneous strips to represent the bottom-depth variation and 35 modes for each strip. To mimic a homogeneous half-space at depth, the absorption increases gradually above a traction-free "false" bottom. Reruns with more strips, a thicker and deeper lying medium truncation at depth, and more modes produced visually identical results.

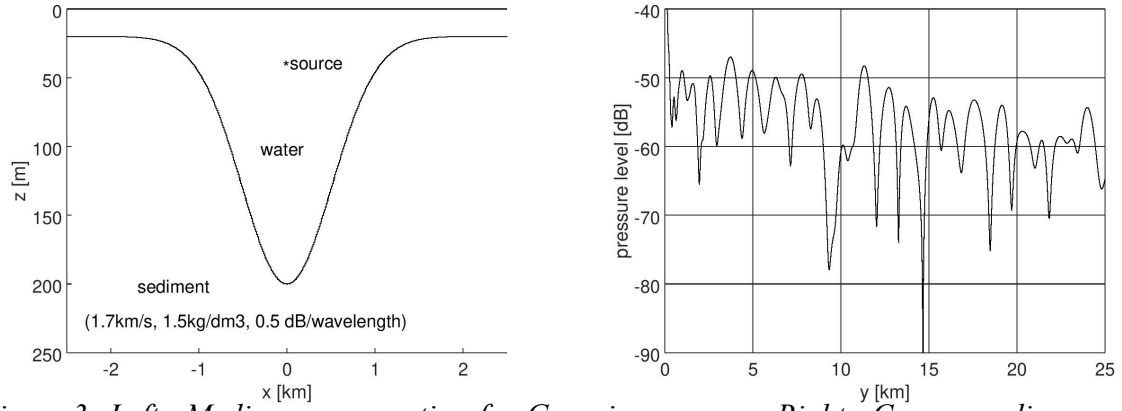

Figure 3: Left: Medium cross-section for Gaussian canyon. Right: Corresponding pressure levels at 25 Hz, in dB re 1 m. Source at $\mathbf{x}_s$ *= (0,0,40) m, receivers at* $\mathbf{x}$ *= (0m,y,30m).*

Fig. 4 shows coupled-mode results for a canyon with a ridge, which provides energy channelling in one half of the canyon and partial shielding of the other. Specify two laterally homogeneous connection strips to define partial waves: -1.5 km $< x <$ -0.250 km (source region) and 0.250 km $< x <$ 1.5 km. There are three surrounding region sequences: A ($x <$ -1.5 km), B ($|x| <$ 0.250 km, for the ridge), and C (1.5 km $< x$). Fig. 5 shows a few of the partial waves.

Partial waves involving several reflections are weak at close y ranges. Plots of reflection-matrix columns as functions of κ/ω, Fig. 6, verify that the modal reflections from the sloping canyon sides and from the ridge are weaker for small κ than for κ-values corresponding to more "grazing-like" incidence. The reflections, as well as the transmission through the ridge (right panel of Fig. 6), may induce significant mode conversion.

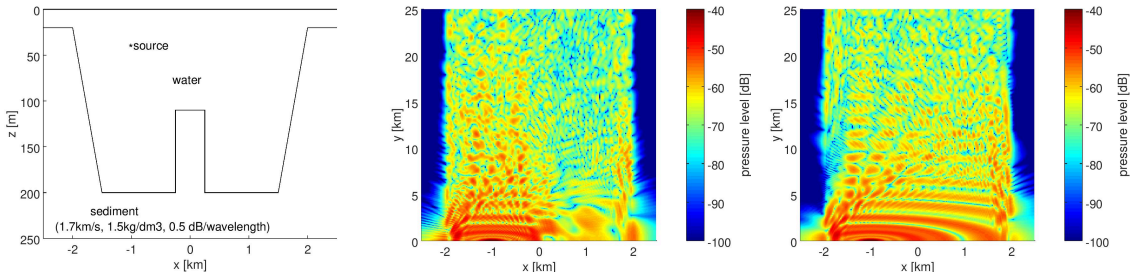

Figure 4: Left: Medium cross-section for canyon with ridge. Middle: Corresponding pressure levels at 25 Hz, in dB re 1 m, using about 70 strips. Source at $\mathbf{x}_s$ *= (-1000,0,40) m, receiver depth 30 m. Right: As middle panel but for canyon without ridge.*

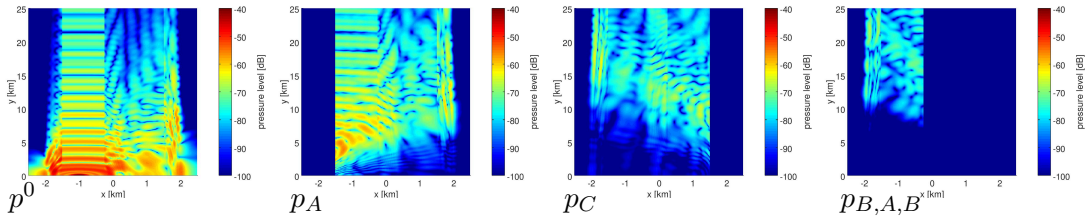

Figure 5: A few partial waves corresponding to the middle panel in Figure 4.

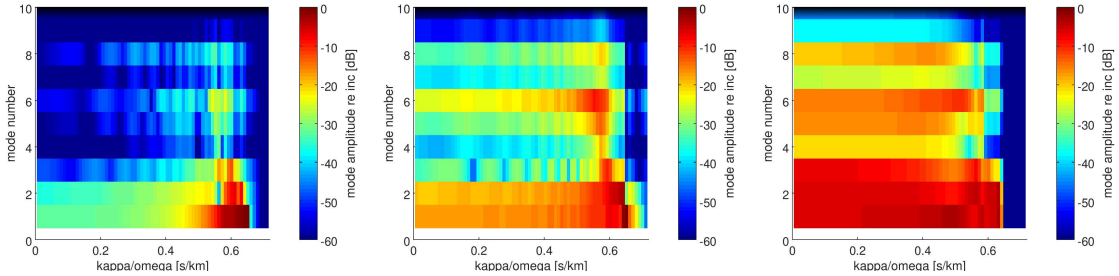

Figure 6: A few modal R/T-matrix columns for the canyon example with a ridge, as functions of κ/ω *with mode 1 as the incident mode. Only the first three modes are propagating. Left: reflection at one of the sloping canyon sides. Middle: reflection at the ridge. Right: transmission through the ridge.*

REFERENCES

[1] S. M. Ivansson, "Multiple underwater sound scattering by cylindrically symmetric anomalies," *J. Acoust. Soc. Am.*, vol. 147, pp. 1429–1440, 2020.

[2] M. Abramowitz and I. A. Stegun, *Handbook of Mathematical Functions*. Washington, D.C.: National Bureau of Standards, 1965.

[3] F. W. J. Olver, "The asymptotic expansion of Bessel functions of large order," *Phil. Trans. R. Soc. Lond. A*, vol. 247, pp. 328–368, 1954.

[4] F. W. J. Olver, *Asymptotics and Special Functions*. New York: Academic Press, 1974.

[5] S. M. Ivansson, "Coupled-mode field computations for media with locally reacting irregular boundaries," *J. Acoust. Soc. Am.*, vol. 150, pp. 2985–2998, 2021.

[6] B. L. N. Kennett, *Seismic Wave Propagation in Stratified Media*. Cambridge: Cambridge University Press, 1983.

[7] K. Lee, W. Seong, and Y. Na, "Split step Padé solver for three-dimensional Cartesian acoustic parabolic equation in stair-step representation of ocean environment," *J. Acoust. Soc. Am.*, vol. 146, pp. 2050–2057, 2019.